On modeling biomolecular–surface nonbonded interactions: application to nucleobase adsorption on single-wall carbon nanotube surfaces

2012 Nanotechnology 23 165703

(http://iopscience.iop.org/0957-4484/23/16/165703)

c a a	*Form Approved* *OMB No. 0704-0188*
A A	
T AT T T	AT C
T T A T T **c a ac b ac ca** **c ba a a b a b ac**	C T ACT G A T G A T
A T	CT TA T
G GA AT A A A **c a c ab a a a a ac** **c a a c a**	G GA AT T
G T G AG C A A A	T AC T T
T T A A A T TAT T **b c a b**	
TA T **a c ( ) ( )**	
A T ACT **c c ba a a c a a** **ca b a b ( ) b c a ca c a c ca a** **c a a ( ) a ( ) ( ) a c ( ) a a a** **a c ( ) ba a c a ( ) ( ) a ( ) c a** **a a a a c c c c a c a c a** **a c a a a c ac b c** **a a c a a a b c a c a ac c c a a** **ca c a a c ba a a ( ) a ( )** **ac a c a c a a a** **a c ac c a c a a a a a** **c a a a (b a** **a c) b c a c ac ca a a a ca** **b a c a a a a a a** **c b b ac c ca b ca a a** **b ca ca c a a a c ba a a c** **a ba a a ac b a c** **c b ca a a b a ac**	
CT T	

C T C A CAT			TAT A T ACT **a a** **( )**	AG	A
T **c a**	A T ACT **c a**	T AG **c a**			

a a ( )
A

Nanotechnology **23** (2012) 165703 (6pp) doi:10.1088/0957-4484/23/16/165703

On modeling biomolecular–surface nonbonded interactions: application to nucleobase adsorption on single-wall carbon nanotube surfaces

B Akdim[1,2], R Pachter[1], P N Day[1,2], S S Kim[1,3] and R R Naik[1]

[1] Materials and Manufacturing Directorate, Air Force Research Laboratory, Wright-Patterson Air Force Base, OH 45433, USA
[2] General Dynamics Information Technology, Incorporated, Dayton OH 45433, USA
[3] UES, Incorporated, Dayton OH 45433, USA

E-mail: Brahim.Akdim@wpafb.af.mil and Ruth.Pachter@wpafb.af.mil

Received 5 October 2011, in final form 6 February 2012
Published 30 March 2012
Online at stacks.iop.org/Nano/23/165703

Abstract
In this work we explored the selectivity of single nucleobases towards adsorption on chiral single-wall carbon nanotubes (SWCNTs) by density functional theory calculations. Specifically, the adsorption of molecular models of guanine (G), adenine (A), thymine (T), and cytosine (C), as well as of AT and GC Watson–Crick (WC) base pairs on chiral SWCNT C(6, 5), C(9, 1) and C(8, 3) model structures, was analyzed in detail. The importance of correcting the exchange–correlation functional for London dispersion was clearly demonstrated, yet limitations in modeling such interactions by considering the SWCNT as a molecular model may mask subtle effects in a molecular–macroscopic material system. The trend in the calculated adsorption energies of the nucleobases on same diameter C(6, 5) and C(9, 1) SWCNT surfaces, i.e. G > A > T > C, was consistent with related computations and experimental work on graphitic surfaces, however contradicting experimental data on the adsorption of single-strand short homo-oligonucleotides on SWCNTs that demonstrated a trend of G > C > A > T (Albertorio *et al* 2009 *Nanotechnology* **20** 395101). A possible role of electrostatic interactions in this case was partially captured by applying the effective fragment potential method, emphasizing that the interplay of the various contributions in modeling nonbonded interactions is complicated by theoretical limitations. Finally, because the calculated adsorption energies for Watson–Crick base pairs have shown little effect upon adsorption of the base pair farther from the surface, the results on SWCNT sorting by salmon genomic DNA could be indicative of partial unfolding of the double helix upon adsorption on the SWCNT surface.

S Online supplementary data available from stacks.iop.org/Nano/23/165703/mmedia

(Some figures may appear in colour only in the online journal)

1. Introduction

The ability to enrich single-wall carbon nanotube (SWCNT) samples by a specific chirality is important in designing materials for improved nanoelectronics, while diameter selectivity could be useful, for example, because of practical considerations [1]. SWCNT sorting with ssDNA has been recently demonstrated based on earlier work [2], in which $d(GT)_n$ (n = 10–45) were used for low-resolution metal/semiconductor and diameter carbon nanotube separation. Selectivity of

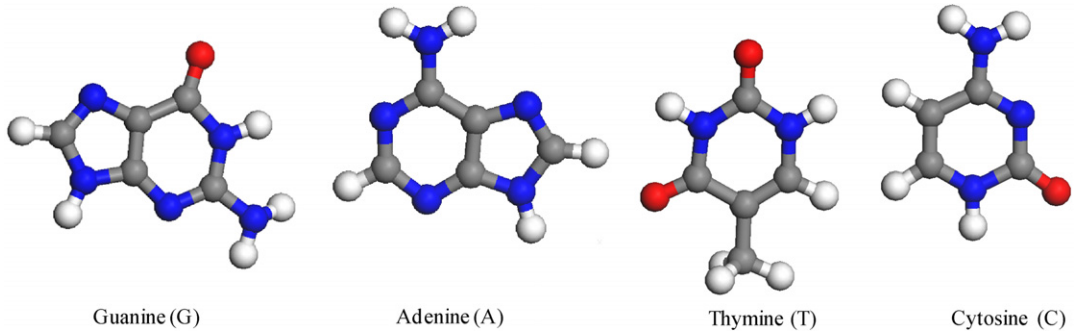

Figure 1. The nucleobases (NBs) considered as mimics for ssDNA adsorption on SWCNTs.

the SWCNT to particular ssDNA sequences, dependent on chirality and diameter, was evident. However, the selectivity in adsorption, even for relatively small diameter SWCNTs, has not been fully explained yet. Although this question was addressed by molecular dynamics (MD) simulations [3], application of an empirical potential is limited because of a lack in the ability to model SWCNT σ–π re-hybridization with diameter or subtle changes in chirality, among other shortcomings. For example, Johnson *et al* claimed [3], based on empirical force-field molecular dynamics (MD) simulations, that nucleotide base (NB)–SWCNT binding is not affected by the chirality of the carbon nanotubes, yet this is contrary to experimental work, in which metallic SWCNTs were noted to be less eluted [2]. Although recently Tu *et al* [4] showed a targeted elution of metallic SWCNTs by a trial-and-error ssDNA mutation approach, a fundamental understanding of intrinsic interactions is still elusive. For example, a metallic C(7, 7) SWCNT was eluted with a modification in TTATTATTATTATT to C, however considering a larger diameter (9.50 versus 7.72 Å) than that of the C(8, 3) SWCNT, thus rendering the two-dimensional wrapping hypothesis unclear. Note that it was shown by MD simulations that solvent and entropic effects are minimal in this case [3]. Modeling of the intrinsic interactions is important also in understanding the enrichment obtained by the use of salmon genomic DNA (SaDNA) for SWCNT separation, as demonstrated by Kim *et al* [5]; SaDNA is an abundant byproduct of the fishing industry and could provide cost savings in large-scale production.

Quantum mechanical calculations provide higher accuracy than empirical force-fields in modeling intrinsic interaction energies, but have been limited so far to zigzag and armchair SWCNT models, performed primarily at levels of theory that may not take into account nonbonded interactions adequately [6–9]. In this work, the objective is to gain an understanding by density functional theory (DFT) calculations of the selectivity of single NBs (guanine (G), adenine (A), thymine (T), and cytosine (C), see figure 1), and of AT and GC Watson–Crick (WC) NB pair model systems, towards adsorption on chiral SWCNT model compounds. Chiral SWCNTs which are known to be enriched experimentally [2], i.e. C(6, 5) (chiral angle 27°) and C(9, 1) (5.2°) with the same diameter, as well as C(8, 3) (15.3°) having a similar diameter, were analyzed, which have not been explored so far theoretically. In this context, we discuss aspects of modeling molecule–inorganic surface interactions, and the limitations encountered in the approach taken. Although a direct comparison of the results with experimentally observed trends in sorting SWCNTs by single-strand hetero-oligonucleotides or double-strand SaDNA is difficult to discern, the calculated NB adsorption energies enabled a qualitative explanation for homo-oligonucleotides, forming the basis for further exploration.

2. Computational methods

2.1. Methods

The frequency-dependent interactions between finite systems can be expressed in terms of the Hamaker constants C_n, i.e. $\Delta E(R) = -\sum_{n=6}^{\infty} \frac{C_n}{R^n}$, where R is their separation. The first term (C_6) for two molecules A and B is given by $C_6^{AB} = \frac{3}{\pi}\int_0^{\infty} du\, \alpha^A(iu)\alpha^B(iu)$, where the polarizability tensors are evaluated at the imaginary frequency iu. Wu and Yang [10] proposed that the exchange–correlation functional can be corrected non-self-consistently by the term $E_{dis} = -f_d(R)\frac{C_6}{R^6}$, where $f_d(R)$ is a damping function, C_6 is based on the polarizability of the constituent atoms, and R^6 defines the asymptotic form of the interaction. It is assumed that quantum mechanical calculations are adequate in describing all except dispersion interactions, dependent on the level of theory employed. Consequently, numerous schemes to include long-range dispersion in DFT functionals for modeling larger systems have been suggested [11, 12]. Notably, Grimme's B97-D has proven quite successful in modeling intermolecular interactions for molecular systems, and is robust because of extensive validation [13].

However, accurate prediction is further complicated in modeling nonbonded molecular–surface interactions. For molecular adsorption on a solid surface at a small distance the Hamaker constant is given by $C = \frac{1}{4\pi}\int_0^{\infty} du\, \alpha(iu)(\frac{\varepsilon(iu)-1}{\varepsilon(iu)+1})$ [14], where $\varepsilon(iu)$ is the frequency-dependent dielectric function at the imaginary frequency. This was shown to be important in modeling interactions between proteins and Si and SiO_2 surfaces [15], where the TDDFT calculated surface dielectric function and the polarizability of the adsorbate were combined. Although predictions of the dielectric response of SWCNTs from first

Table 1. Nearest distances (Å) of heavy atoms in NBs from the SWCNT surface.

	C–SWCNT	N–SWCNT	O–SWCNT
G			
C(6, 5)	3.02	3.17	3.57
C(9, 1)	3.11	3.06	3.40
C(8, 3)	3.00	3.20	3.60
A			
C(6, 5)	3.12	3.12	N/A
C(9, 1)	3.10	3.23	N/A
C(8, 3)	3.12	3.12	N/A
T			
C(6, 5)	3.11	3.15	3.24
C(9, 1)	3.18	3.22	3.29
C(8, 3)	3.12	3.27	3.24
C			
C(6, 5)	3.10	3.23	3.38
C(9, 1)	3.12	3.06	3.51
C(8, 3)	3.06	3.26	3.26

principles have been reported [16, 17], theoretical work is still lacking. This could explain, in part, the weaker adsorption of metallic SWCNTs that are less eluted by ssDNA, as observed experimentally [2]. In seeking qualitative trends for NB adsorption on chiral SWCNTs, in this work we assume that the solid's polarizability can be approximated by those of the constituent atoms. The functional B97-D was applied in our work, and, for comparison, the EFP2 method [18] which has not been applied as yet to model NB–SWCNT interactions. This method provides a better understanding because the interaction energy is determined as a sum of electrostatic, Pauli exchange, polarization, dispersion, and charge transfer terms consistently after first principles [18]. The combination of results from the two methods provided insight into the interplay of electrostatic and London dispersion interactions for NB adsorption on chiral SWCNTs.

2.2. Computational details

To ensure that no artifacts in the starting configuration of NB adsorption on the SWCNT occurred, simulations at 300 K for 1 ps were carried out with the self-consistent charge density functional tight-binding (SCC-DFTB) scheme using an empirical correction to the dispersion (DFTB-D, mio-01 parameters) [19–21] and an Anderson thermostat. Structures were then optimized with B97-D/6-31G* [13, 22]. Note that the translational unit cells for the chiral SWCNTs contain 388 and 364 carbon atoms for C(8, 3), and C(6, 5) and C(9, 1), respectively, too large for feasible computations, and therefore about half of the unit cell was used, specifically 167 and 161 atoms, respectively. Calculations with EFP2/6-31G were performed for C(5, 0) because of the system size, where the starting structures were optimized at the B97-D/6-31G* level. To mimic dsDNA adsorption, calculations for WC models of base pairs (AT and GC) and of double base pairs (ATAT and ATGC) were carried out. All calculations were performed with Gaussian09 [23] except for EFP2 with GAMESS [24].

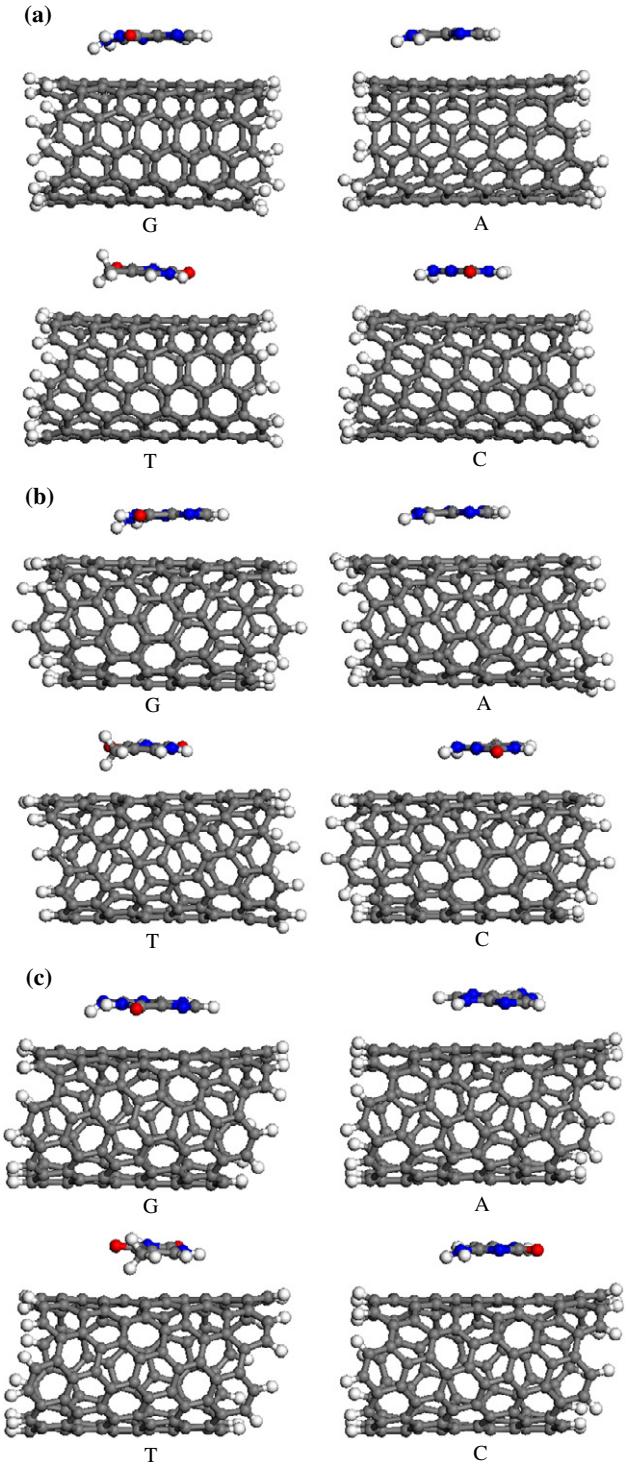

Figure 2. Structures of systems with NBs adsorbed on (a) C(6, 5), (b) C(9, 1) and (c) C(8, 3) SWCNTs.

3. Results and discussion

The geometrical parameters of the optimized SWCNT–NB molecular systems are listed in table 1. The results show stabilized stacking of the NBs on the SWCNT surface (see figure 2). π-stacking of DNA NBs on surfaces is well known, as demonstrated experimentally, for example

Table 2. Adsorption energies E_{ads} (kcal/mol) for NBs and WC base pairs adsorbed on SWCNTs (B97-D/6-31G*). (Note: E_{ads} values were systematically decreased by about 15–17 kcal mol^{-1} for single point calculations (B97-D/Def2-TZVP).)

NB	C(6, 5)	C(9, 1)	C(8, 3)
G	−20.72	−20.36	−20.96
A	−16.99	−16.79	−16.66
C	−14.64	−14.20	−15.72
T	−15.18	−14.59	−14.85
WC NB base pair	C(6, 5)	C(9, 1)	C(8, 3)
AT	−28.51	−27.57	−29.03
GC	−29.66	−29.01	−29.05

for adenine adsorption on graphite [25], and by empirical force-field simulations ([26] and references therein), where the potentials were extensively parameterized for London dispersion interactions. We note that for the SWCNT chiralities considered, the distances of the NBs' carbon, nitrogen and oxygen atoms from the surface were 3.0–3.2 Å, 3.2–3.3 Å, 3.3–3.6 Å, respectively, with an average nearest neighbor distance of ca. 3.2 Å, consistent with B97-D results for NBs adsorbed on graphene and for π-stacked NBs [27]. The values are somewhat larger than those calculated with the M0-2X [28] functional for NBs adsorbed on armchair SWCNTs [9] and zigzag C(10, 0) [7], presumably because of the lack of an explicit dispersion correction. Notably, calculations carried out with the PBE functional resulted in non-stacked NB structures on the SWCNT. A vertical positioning for the NB relative to the SWCNT surface was obtained for T on C(6, 5), a tilted positioning for C on C(6, 5), and similarly for the G and A NBs on C(8, 3) (figure S1 in supplementary data available at stacks.iop.org/Nano/23/165703/mmedia). Interestingly, a different behavior for the pyrimidine-based NBs (C and T) and purine-based (G and A) structures for varying chiralities was shown, which may influence the affinity towards self-stacking in water [29]; this is, however, beyond the scope of this study.

Adsorption energies were calculated from $E_{ads} = E(\text{SWCNT} - \text{NB}) - E(\text{SWCNT}) - E(\text{NB})$, as summarized in table 2. Results for C(5, 0), for comparison with previous work but here using B97-D, were calculated as −19.2, −15.0, −14.8 and −13.8 kcal mol^{-1} for G, A, T, C, respectively. The trend in the calculated adsorption energies of the NBs on same diameter C(6, 5) and C(9, 1), and on C(5, 0), was predicted as G > A > T > C, consistent with previously calculated values for graphene and C(5, 0) [8, 9, 27]. The E_{ads} values were lower for a higher SWCNT curvature because of a smaller contribution of dispersion. The predicted adsorption trend is consistent with experiments on the interaction of ssDNA on a graphitic surface [30, 31]. Similarly, the C(8, 3) results are consistent with isothermal titration calorimetry values, using samples of graphene, where in the order of G > A > C > T the positions of C and T seemed to be interchangeable [32]. Note that the values of E_{ads} were systematically decreased by about 15–17 kcal mol^{-1} for single point B97-D/Def2-TZVP calculations, but the adsorption trend did not change. Furthermore, our qualitative agreement for C(6, 5) with the results of Antony *et al* [27] for which larger graphene sheet models showed the same trend, implies that this relation will not be affected by an increase of the already relatively large chiral SWCNT model systems. The order of adsorption strength for the C and T is reversed for C(8, 3) compared to C(6, 5) and C(9, 1) (table 2), however of a slightly different diameter. The dispersion contributions for C(6, 5) and C(8, 3) showed a similar trend, e.g. for C(6, 5): −27.50, −25.10, −22.70, −20.50; C(8, 3): −28.20, −23.00, −22.20, −21.9 kcal mol^{-1}, for G, A, T, C, respectively. The trend can be explained by the relative polarizabilities of the NBs for a given carbon-based nanostructure. The results of the relative trend are indeed consistent with the trend in the experimentally determined ionization potentials of the NBs that were compiled by Roca-Sanjuán *et al* [33]. This trend may also be related to the so-called π-misalignment [34] in SWCNTs of varying chirality.

Table 3. Adsorption energies E_{ads} (kcal mol^{-1}) of NBs adsorbed on C(5, 0) using EFP2.

	G	A	T	C
Electrostatic	−5.89	−1.82	−3.98	−4.02
Repulsion	6.72	4.09	8.29	5.68
Polarization	−3.17	−0.64	−3.20	−3.49
Dispersion	−24.15	−19.04	−27.20	−19.67

At the same time, recent experimental data for single-strand homo-oligonucleotides, $d(A)_{12}$, $d(T)_{12}$, $d(C)_{12}$ and $d(G)_{12}$, exhibited a different trend in adsorption, where a stability order of G > C > A > T was observed [35]. This was explained in terms of electrostatic interactions between the phosphate backbone and the aqueous environment, or base stacking within a single strand due to changes in the SWCNTs as compared to a flat graphitic surface; this is, however, still not fully elucidated. It is interesting to point out that the EFP2 results (see table 3) demonstrated a similar trend of G > C > A > T in adsorption energies upon exclusion of dispersion interactions (which may not be accurately calculated in EFP from TDHF [36]). The complexity of the theoretical approximations is thus highlighted, and we also note that, although adsorption is primarily driven by π–π stacking, the experimental environment may affect the order of adsorption.

The enrichment of C(6, 5) using genomic SaDNA [5] demonstrated an important advantage practically, and therefore an understanding of the intrinsic adsorption energies could provide a first step towards further exploration of such hybrid materials. Optimized AT and GT WC base pairs and the corresponding structures adsorbed on SWCNTs are shown in figures 3(a) and (b), respectively. The calculated and experimental geometries [37] of the WC base pairs are consistent with our results (summarized in table 4). Upon adsorption on the SWCNTs, curving of the WC base pairs from planarity to maximize dispersion interactions is demonstrated in figure 3(b). The effects of adsorption on the hydrogen bonding in the WC base pair are small, although slightly larger for C(8, 3) than for C(6, 5). Note that the adsorption energies in this case are non-additive, namely the adsorption energies of G and C do not add up to those of

Table 4. Intermolecular distances (Å) in AT and GC base pairs using B97-D/6-31G*.

AT base pair					
	N6–O4	N1–N3	H6–O4	N1–H3	H2–O2
AT	2.92	2.82	1.90	1.77	2.76
Adsorbed on C(6, 5)	2.92	2.83	1.91	1.81	2.68
Adsorbed on C(8, 3)	2.88	2.75	1.95	1.73	2.66
GC base pair					
	O1–N1	N2–N2′	N3–O3	O1–H1	H2–N2′
GC	2.79	2.92	2.92	1.74	1.88
Adsorbed on C(6, 5)	2.81	2.92	2.88	1.78	1.91
Adsorbed on C(8, 3)	2.82	2.91	2.90	1.77	1.88

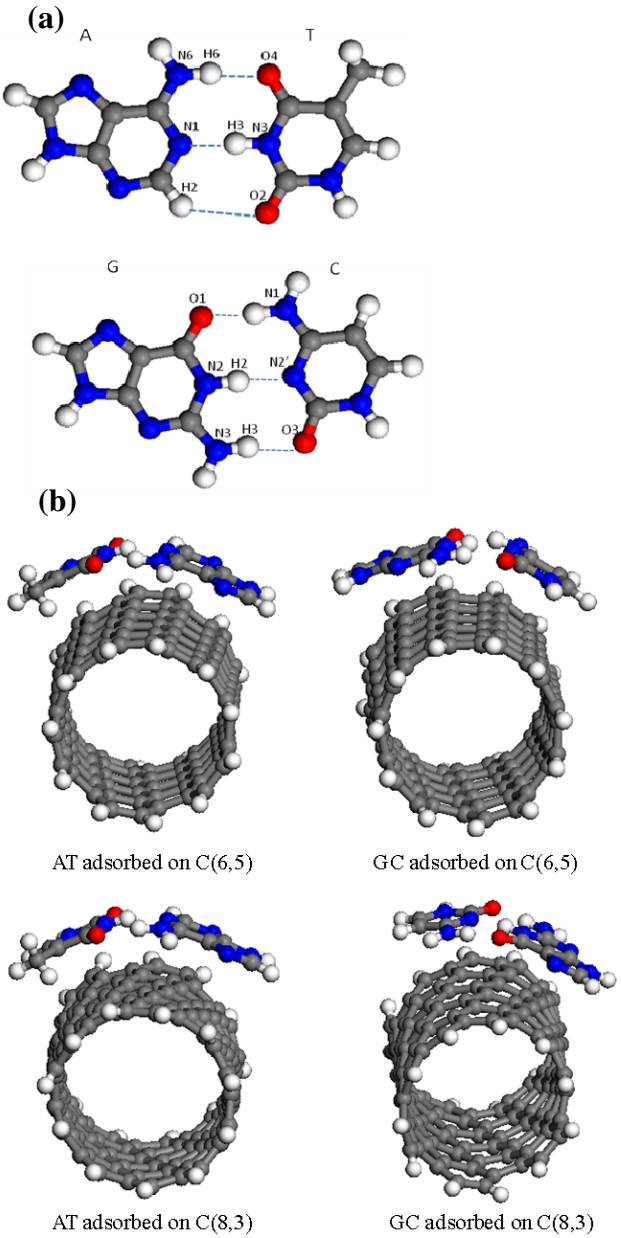

Figure 3. Hydrogen bonding for (a) WC base pairs AT and GC, and (b) base pairs adsorbed on C(6, 5), C(9, 1), and C(8, 3) SWCNTs.

a GC WC base pair. This is due to the hydrogen bonding within the WC base pair that changes the electronic structure and strength of adsorption. For example, the Mulliken partial atomic charges of G and C separately adsorbing on C(8, 3) are 0.01e, while the respective value for a GC WC base pair is 0.04e. For further validation, in mimicking experimental characteristics, calculations of a double stack were also carried out, assumed to maintain the twist of the double helix in the dsDNA (see figure S2 available at stacks.iop.org/Nano/23/165703/mmedia). The double base pair adsorption interaction energies demonstrated the same trend as the single WC base pairs (representative adsorption energy results are shown in figure S3 available at stacks.iop.org/Nano/23/165703/mmedia), indicating that the adsorption is not affected by base pairs that are positioned further away from the SWCNT surface. However, upon possible partial unfolding of the double helical structure in a realistic environment even stronger adsorption is expected, thus motivating future exploration of SWCNT dispersion with genomic salmon DNA.

4. Conclusion

In this work we reported calculations of NB adsorption on chiral C(6, 5), C(9, 1), and C(8, 3) SWCNTs to elucidate trends in the intrinsic nonbonded interactions. Although the geometries of the hybrid material model structures were qualitatively consistent with previous work, the importance of correcting the exchange–correlation functional for dispersion was clearly demonstrated. Limitations in modeling the dispersion interactions by considering the SWCNT as a molecular model may mask subtle effects in a molecular–macroscopic system.

The trend in calculated adsorption energies of the NBs on same diameter C(6, 5) and C(9, 1) SWCNT surfaces was predicted as G > A > T > C, which is consistent with related computations and experimental work on graphitic surfaces. The calculated dispersion contributions followed this trend, explained by the relative polarizability of the NBs for a given carbon-based nanostructure. The order of adsorption strength for the C and T NBs was reversed for C(8, 3), which is difficult to assess in a direct comparison because of change in diameter. However, recent experimental data on the adsorption of single-strand short homo-oligonucleotides on SWCNTs demonstrated a trend of G > C > A > T [35]. The possible importance of electrostatic interactions was partially captured by the EFP2 results when excluding the dispersion contribution, which was calculated at the TDHF level, to be

improved upon in future work. Finally, because the calculated adsorption energies for Watson–Crick base pairs have shown little effect upon adsorption of the base pair farther from the surface, the results on SWCNT sorting by SaDNA could be indicative of partial unfolding of the double helix upon adsorption on the surface.

Acknowledgments

The DoD High Performance Computing Modernization Program is gratefully acknowledged for computational resources and the AFRL Distributed Shared Resource Center for helpful support.

References

[1] Zhang L, Tu X, Welsher K, Wang X, Zheng M and Dai H 2009 *J. Am. Chem. Soc.* **131** 2454–5
[2] Tu X, Manohar S, Jagota A and Zheng M 2009 *Nature* **460** 250–3
[3] Johnson R R, Johnson A T C and Klein M L 2010 *Small* **6** 31–4
[4] Tu X-M, Hight W A R, Khripin C Y and Zheng M 2011 *J. Am. Chem. Soc.* **133** 12998–3001
[5] Kim S N, Kuang Z, Grote J G, Farmer B L and Naik R R 2008 *Nano Lett.* **8** 4415–20
[6] Wang H and Ceulemans A 2009 *Phys. Rev.* B **79** 195419
[7] Stepanian S G, Karachevtsev M V, Glamazda A Y, Karachevtsev V A and Adamowicz L 2009 *J. Phys. Chem.* A **113** 3621–9
[8] Gowtham S, Scheicher R H, Pandey R, Karna S P and Ahuja R 2008 *Nanotechnology* **19** 125701
[9] Umadevi D and Sastry G N 2011 *J. Phys. Chem. Lett.* **2** 1572–6
[10] Wu Q and Yang W 2002 *J. Chem. Phys.* **116** 515–24
[11] Johnson E R, Mackie I D and Di L G A 2009 *J. Phys. Org. Chem.* **22** 1127–35
[12] Riley K E, Pitonak M, Jurecka P and Hobza P 2010 *Chem. Rev.* **110** 5023–63
[13] Antony J and Grimme S 2006 *Phys. Chem. Chem. Phys.* **8** 5287–93
[14] Zaremba E and Kohn W 1976 *Phys. Rev.* B **13** 2270–85
[15] Oliveira M J T, Botti S and Marques M A L 2011 *Phys. Chem. Chem. Phys.* **13** 15055–61
[16] Spataru C D, Ismail-Beigi S, Benedict L X and Louie S G 2004 *Phys. Rev. Lett.* **92** 077402
[17] Marinopoulos A G, Reining L and Rubio A 2008 *Phys. Rev.* B **78** 235428
[18] Gordon M S, Slipchenko L, Li H and Jensen J H 2007 *Annu. Rep. Comput. Chem.* **3** 177–93
[19] Elstner M, Porezag D, Jungnickel G, Elsner J, Haugk M, Frauenheim T, Suhai S and Seifert G 1998 *Phys. Rev.* B **58** 7260–8
[20] Frauenheim T, Seifert G, Elstner M, Niehaus T, Kohler C, Amkreutz M, Sternberg M, Hajnal Z, Di C A and Suhai S 2002 *J. Phys.: Condens. Matter* **14** 3015–47
[21] Elstner M, Hobza P, Frauenheim T, Suhai S and Kaxiras E 2001 *J. Chem. Phys.* **114** 5149–55
[22] Grimme S 2006 *J. Comput. Chem.* **27** 1787–99
[23] Gaussian 09 R A *et al* 2009 *Gaussian, Inc.* Wallingford CT
[24] Schmidt M W *et al* 1993 *J. Comput. Chem.* **14** 1347–63
[25] Freund J E, Edelwirth M, Kroebel P and Heckl W M 1997 *Phys. Rev.* B **55** 5394–7
[26] Roxbury D, Jagota A and Mittal J 2011 *J. Am. Chem. Soc.* **133** 13545–50
[27] Antony J and Grimme S 2008 *Phys. Chem. Chem. Phys.* **10** 2722–9
[28] Zhao Y and Truhlar D G 2008 *Theor. Chem. Acc.* **120** 215–41
[29] Hughes J M, Cathcart H and Coleman J N 2010 *J. Phys. Chem.* C **114** 11741–7
[30] Manohar S, Mantz A R, Bancroft K E, Hui C-Y, Jagota A and Vezenov D V 2008 *Nano Lett.* **8** 4365–72
[31] Sowerby S J, Cohn C A, Heckl W M and Holm N G 2001 *Proc. Natl Acad. Sci. USA* **98** 820–2
[32] Varghese N, Mogera U, Govindaraj A, Das A, Maiti P K, Sood A K and Rao C N R 2009 *ChemPhysChem* **10** 206–10
[33] Roca-Sanjuan D, Rubio M, Merchan M and Serrano-Andres L 2006 *J. Chem. Phys.* **125** 084302
[34] Niyogi S, Hamon M A, Hu H, Zhao B, Bhowmik P, Sen R, Itkis M E and Haddon R C 2002 *Acc. Chem. Res.* **35** 1105–13
[35] Albertorio F, Hughes M E, Golovchenko J A and Branton D 2009 *Nanotechnology* **20** 395101
[36] Adamovic I and Gordon M S 2005 *Mol. Phys.* **103** 379–87
[37] Zhou P-P and Qiu W-Y 2009 *J. Phys. Chem.* A **113** 10306–20